

EUV Wave and Coronal Seismology

Pooja Devi¹, Ramesh Chandra¹, Arun Kumar Awasthi², Brigitte Schmieder^{3,4},
Reetika Joshi^{5,6}

¹Department of Physics, DSB Campus, Kumaun University, Nainital 263001, India

²Space Research Centre, Polish Academy of Sciences, Bartycka 18A, 00-716 Warsaw, Poland

³LIRA, Observatoire de Paris, CNRS, Université de Paris, 5 place Janssen, 92290 Meudon, France

⁴Centre for mathematical Plasma Astrophysics, Dept. of Mathematics, KU Leuven, 3001 Leuven, Belgium

⁵Roseland Centre for Solar Physics, University of Oslo, P.O. Box 1029 Blindern, N-0315 Oslo, Norway

⁶Institute of Theoretical Astrophysics, University of Oslo, P.O. Box 1029 Blindern, N-0315 Oslo, Norway
Email: setiapooja.ps@gmail.com

Abstract. We present an investigation of the Extreme-Ultraviolet (EUV) wave linked to the flare that occurred on 28 October 2021, along with the associated coronal loop oscillation and type II radio burst. The EUV wave was observed by multi-viewpoint with Solar Dynamics Observatory and Solar Terrestrial Relations Observatory – A. The associated coronal mass ejection (CME) was observed by Large Angle and Spectrometric Coronagraph (LASCO) as well by COR1 coronagraph. From the multi-view observation, we found that the EUV wave is propagated ahead of the connected CME. The coronal magnetic field measurement was performed by the coronal loop oscillations as well by the associated m-type II radio burst observations. We found the magnetic field strength values computed by both methods are consistent and are in the range of ≈ 5 to 10 G.

Keywords. EUV wave, Coronal Mass Ejection, Loop Oscillations, m-Type II Radio Burst

1. Introduction

During the campaign of $H\alpha$ observation in 1960, [Moreton and Ramsey \(1960\)](#) found the large scale moving disturbances on the solar chromosphere. Later these disturbances were named as “Moreton waves”. Their reported speed is in the range of 500 to 2000 km s⁻¹ (see reviews by [Warmuth 2015](#); [Chen 2016](#)). The generation of Moreton waves is due to the fast mode magnetohydrodynamic (MHD) shock sweeping into the chromosphere. [Thompson et al. \(1998\)](#) observed similar propagating features in 195 Å wavelength with Extreme-ultraviolet Imaging Telescope (EIT; [Delaboudinière et al. 1995](#)) onboard Solar and Heliospheric Observatory (SOHO; [Domingo et al. 1995](#)) and named them as “EIT waves”. Because of their clear visibility in Extreme-ultraviolet (EUV) wavelengths, they are popularly known as “EUV waves” and their speed ranges from a few hundreds to multiple of thousand km s⁻¹.

Initially, these waves were observed with low-cadence data of SOHO and Solar Terrestrial Relations Observatory (STEREO) satellites ([Thompson et al. 1999](#); [Zhukov and Auchère 2004](#); [Zhukov et al. 2009](#)) and were proposed to be the fast-mode MHD waves. However, after analyzing the high spatio-temporal data of Solar Dynamics Observatory (SDO), two components (slow, speed is as low as 10 km s⁻¹ and fast (speed can be up to multiple of 1000 km s⁻¹) as well as stationary fronts of this phenomena were reported ([Chen and Wu 2011](#); [Asai et al. 2012](#); [Chandra et al. 2016, 2018, 2021](#)). The observed features can be explained by the hybrid model proposed by [Chen et al. \(2002, 2005\)](#). According to this model, a piston-driven shock forms along the expanding flux rope during its eruption, sweeping the whole solar surface. The legs of the shock produce fast-mode EUV waves. On the other hand, the slower (or

nonwave) component, forms due to successive opening or stretching of the magnetic field lines straddling over the erupting flux rope.

When the coronal mass ejection (CME) propagates out of the solar surface, it produces a shock wave and it is believed that this shock wave could be responsible for the EUV wave disturbances (Biesecker et al. 2002). There are studies, where people try to look into the association between the EUV waves and CMEs and it is found that these two physical phenomena are closely associated (Chen 2009; Dai et al. 2010; Schmieder et al. 2013; Nitta et al. 2014; Muhr et al. 2014). Another evidence of the shock wave is the type II radio bursts observed in coronal heights and can be associated with the EUV waves.

When the fast component of the EUV wave encounters the surrounding magnetic structures, these structures can become unstable. These magnetic structures can be filament or coronal loops. As a result of this instability, these structures can oscillate and be used for the coronal seismology (Warmuth and Mann 2005; Ballai 2007; Guo et al. 2015; Luna et al. 2017; Fulara et al. 2019; Shen et al. 2019; Devi et al. 2022).

In this article, we present an EUV wave from 28 October 2021, associated with a large GOES X1.0 eruptive solar flare, nearby loop oscillations, and a type II radio burst. Section 2 covers the observational data sources and the results. The summary of the article is provided in Section 3.

2. Observations

The EUV wave event of 28 October 2021 was observed by several space based telescopes and its counterpart i.e., Moreton wave, by ground based instruments. We analyse the data of Atmospheric Imaging Assembly (AIA; Lemen et al. 2012) onboard Solar Dynamics Observatory (SDO; Pesnell et al. 2012) and Global Oscillation Network Group (GONG; Harvey et al. 2011) from Earth view and by Extreme-ultraviolet Imager (EUVI) and coronagraphs (COR1) onboard ahead spacecraft of Solar Terrestrial Relations Observatory (STEREO-A; Kaiser et al. 2008) from a different view angle. The radio emission due to this event were observed by e-Callisto spectrographs at Birr Castle, Ireland (BIR) and also by ORFEES (Hamini et al. 2021) at Nançay Radio Observatory. The EUV wave event is accompanied by one of the major GOES X1.0 class two ribbon flare and filament eruption, which produced a ground level enhancement (GLE). The origin of the activities was from NOAA AR 12887, which was located at S26W07 on 28 October 2021. The studies have been done on different activities produced by this event which include: different features of the EUV and Moreton wave (Hou et al. 2022; Devi et al. 2022), solar energetic particles (Kouloumvakos et al. 2024) and related radio bursts (Klein et al. 2022), and GLE (Mavromichalaki et al. 2022; Papaioannou et al. 2022; Mishev et al. 2024). Along with the observations, data-driven simulations of the event are performed by Guo et al. (2023).

2.1. Morphology of EUV Wave and associated CME

The EUV wave appeared on the solar disk $\sim 15:25$ UT in a circular shape. The propagating EUV wave was promptly visible in the northward and fainter in the southward direction. Figure 1 displays base difference snapshots of the wave in different wavelengths. The kinematics of the wave were done by Devi et al. (2022) and Hou et al. (2022) using the time-distance technique. Two components (i.e., fast-mode and nonwave) of the EUV wave were observed. The speed of the nonwave component was found to be ≈ 280 km s⁻¹ and fast-mode ranges from ≈ 550 to 720 km s⁻¹. The speed of the Moreton wave observed in H α was found in the range of ≈ 310 to 540 km s⁻¹.

The EUV wave was associated with a halo CME of linear speed 1519 km s⁻¹ and an acceleration of -61 m s⁻² as reported by the LASCO CME catalog. The CME was also observed by the STEREO-A COR1 coronagraph. In the STEREO-A data, the event is observed close

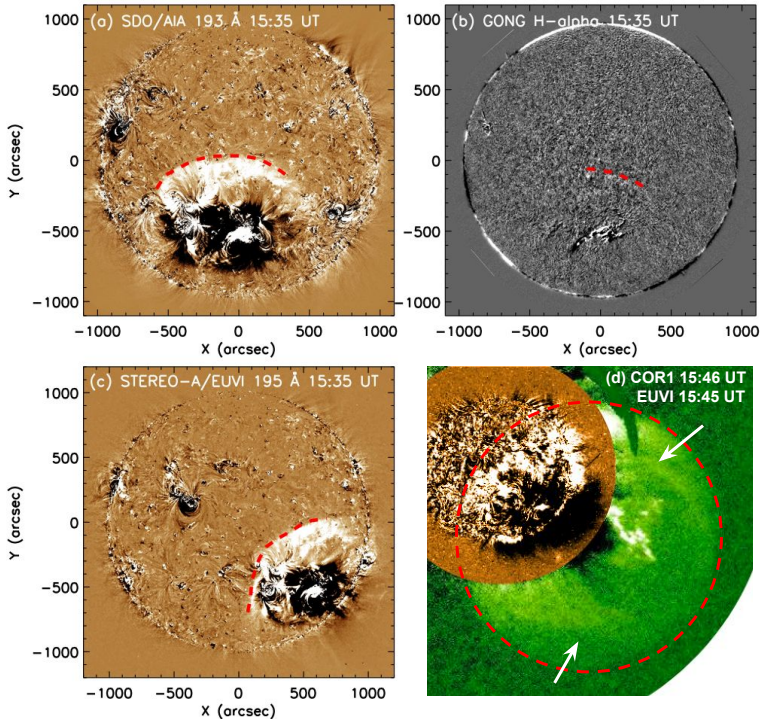


Figure 1. Panel (a, c): Snapshots of the EUV waves observed in AIA 193 Å, and STEREO-A 195 Å. Panel b: H α Observation of GONG, where Moreton wave is visible. panel (d): Overlay of CME observed by COR1 with the STEREO-A data. The red dashed curves in panels (a – c) and the circle in panel (d) are the fronts of the wave. The white arrows in panel (d) show the CME leading edge. (Panels (a) and (d) are adapted and recreated from [Devi et al. 2022](#)).

to the western limb, which provides us to an excellent opportunity to compare spatially these two phenomena. For this comparison, the image of EUVI is overlaid on the COR1 image as shown in Figure 1(d). The internal yellow part is the EUVI 195 Å image at 15:45 UT and the outer green part is the COR1 image at 15:46 UT. Assuming the spherical structure of the EUV wave, we fitted a circle at the outer edge of the EUV wave (shown by a red dashed circle) as suggested by [Gopalswamy et al. \(2013\)](#). The alignment between the EUVI and COR1 images evidenced that the EUV wave was traveling ahead of the CME. This result is confirmed by the data-driven simulation of [Guo et al. \(2023\)](#) (see their Figure 10).

2.2. Loop Oscillations

During the propagation of the EUV wave in the north direction, it encountered the neighboring coronal loops and triggered them to oscillate. The oscillations of two loop systems have been studied in detail by [Devi et al. \(2022\)](#). They computed the periods of loop oscillations using the wavelet method and by fitting a damped sinusoidal function given in their equation 1. The periods from both these methods are found to be consistent with each other and are in the range from 230 to 280 sec. They also calculated the densities inside (n_{in}) and outside (n_{out}) the oscillating loops using the Differential Emission Measure (DEM; [Cheung et al. 2015](#)) technique which are found in the range $1.6 \times 10^8 - 2.1 \times 10^8 \text{ cm}^{-3}$ and $1 \times 10^8 - 1.8 \times 10^8 \text{ cm}^{-3}$, respectively. Oscillations in one of the loop systems along with its periodic analysis are presented in Figure 2. Further, [Devi et al. \(2022\)](#) calculated the coronal magnetic field strength

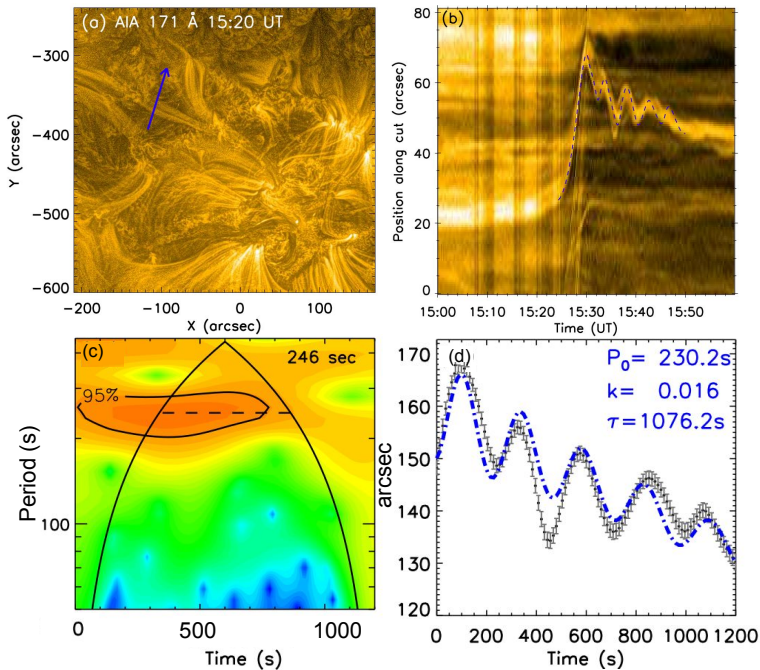


Figure 2. AIA 171 Å image with the clearly observed oscillating loop system is depicted in (a) panel. The direction of oscillation is in the blue arrow direction. The time-slice plot showing the oscillations is shown in (b) panel. The wavelet analysis along with the temporal evolution of oscillation (overlaid by dashed lines) is displayed in panel (c) and (d) panel of the figure. (Adapted from [Devi et al. \(2022\)](#))

(B) using the following equation ([Roberts et al. 1984](#)),

$$B = \frac{L}{P} \sqrt{8\pi\mu m_p n_{in} \left(1 + \frac{n_{out}}{n_{in}}\right)} \quad (1)$$

where, μ is the average molecular weight for coronal abundances, and m_p is mass of proton. Putting all the above values along with the length (L) of oscillating loop (115 – 175 Mm), the B found to vary from ≈ 5.7 to 8.8 G.

2.3. Type II Radio Burst

The event was also associated with type II radio bursts in metric (m) and decametric-hectometric frequency range. The detailed study about the observed type II burst was investigated by [Klein et al. \(2022\)](#) (see their figures 2, 5, and 12). They computed the speed of m-type II burst in the range 1900 – 2600 km s⁻¹. The observed metric type II radio burst is presented in Figure 3. The type II radio burst shows the harmonic and fundamental structures. The splitting in the harmonic structure is observed in ORFEES dynamic spectra. Such splitting in the harmonic band is due to the consequence of the plasma emission of the upstream and downstream shock regions and it was initially interpreted by [Smerd et al. \(1974\)](#). The frequency of observed upstream (f_u) and downstream (f_l) are 173 and 130 MHz, respectively. Using the parameters of harmonic band splitting of m-type II bursts [Klein et al. \(2022\)](#) calculated the Alfvén Mach number (M_A) which is 1.6. Now, using the parameters computed by them, we have calculated B by the following formula ([Vasanth et al. 2014](#)),

$$B = 5.1 \times 10^{-5} \times v_a \times f_l, \quad (2)$$

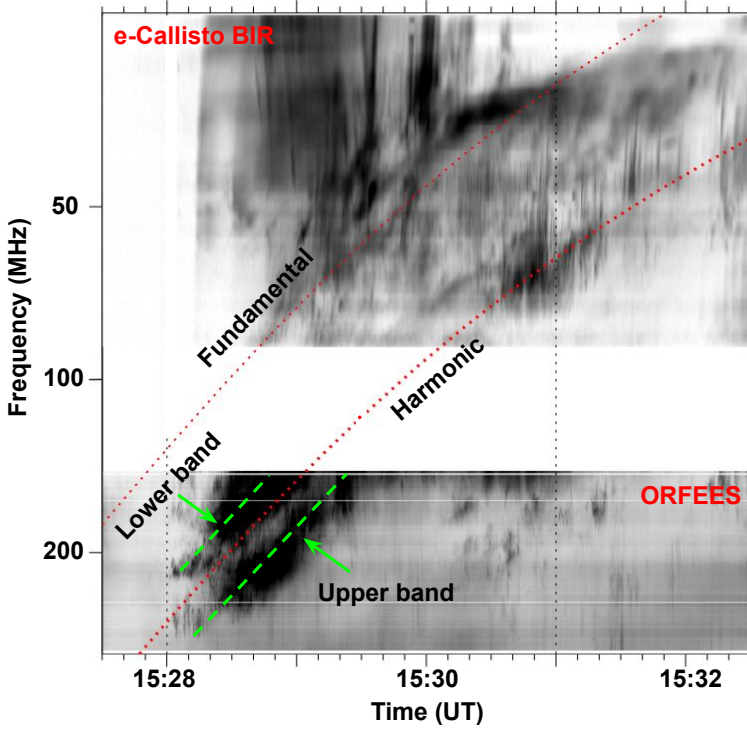


Figure 3. Type II radio bursts in metric range by combining the dynamic spectra from BIR (e-Callisto at Birr Castle, Ireland) and ORFEES. The fundamental and harmonic emissions are shown by red dotted curves. The splitted upper and lower bands of harmonic emission are denoted with green arrows. (Adapted and reformed from Klein et al. (2022))

where the Alfvén speed ($v_a = v_s/M_A$) found to vary from 1187 to 1625 km s⁻¹. Inserting the values of v_a and f_i in equation 2, the computed B is found in the range $\approx 7 - 10$ G, which is consistent with B calculated using the loop oscillation parameters (Section 2).

3. Summary

The EUV wave of 28 October 2021 showed both the fast-mode and nonwave components which can be explained by the hybrid model proposed by Chen et al. (2002). Our analysis revealed that the EUV wave travels in front of the CME leading edge implying that the EUV wave is driven by the CME and not by the flare pressure pulse (Vourlidis and Ontiveros 2009; Kwon et al. 2014; Kwon and Vourlidis 2017; Guo et al. 2023). An important characteristic of this EUV wave is its association with the neighbouring loop oscillations and the type II radio bursts. We have computed the coronal magnetic field using the loops oscillation parameters which are 5.7 – 8.8 G and by the m-type II radio observations harmonic band splitting, the computed value is about 7 – 10 G. The computed B from both these methods are consistent with each other and in the range of previous studies (Nakariakov and Ofman 2001; Aschwanden and Schrijver 2011; Guo et al. 2015; Su et al. 2018; Zhang et al. 2022).

References

- Asai, A., Ishii, T. T., Isobe, H., et al. 2012, *ApJL*, 745(2), L18.
 Aschwanden, M. J. & Schrijver, C. J. 2011, *ApJ*, 736(2), 102.
 Ballai, I. 2007, *Solar Phys.*, 246(1), 177.
 Biesecker, D. A., Myers, D. C., Thompson, B. J., et al. 2002, *ApJ*, 569(2), 1009.

- Chandra, R., Chen, P. F., Fulara, A., et al. 2016, *ApJ*, 822(2), 106.
- Chandra, R., Chen, P. F., Joshi, R., et al. 2018, *ApJ*, 863(2), 101.
- Chandra, R., Démoulin, P., Devi, P., et al. 2021, *ApJ*, 922(2), 227.
- Chen, P. F. 2009, *ApJL*, 698(2), L112.
- Chen, P. F. 2016, *Washington DC American Geophysical Union Geophysical Monograph Series*, 216, 381.
- Chen, P. F., Fang, C., & Shibata, K. 2005, *ApJ*, 622(2), 1202.
- Chen, P. F., Wu, S. T., Shibata, K., & Fang, C. 2002, *ApJL*, 572(1), L99.
- Chen, P. F. & Wu, Y. 2011, *ApJL*, 732(2), L20.
- Cheung, M. C. M., Boerner, P., Schrijver, C. J., et al. 2015, *ApJ*, 807(2), 143.
- Dai, Y., Auchère, F., Vial, J. C., et al. 2010, *ApJ*, 708(2), 913.
- Delaboudinière, J. P., Artzner, G. E., Brunaud, J., et al. 1995, *Solar Phys.*, 162(1-2), 291.
- Devi, P., Chandra, R., Awasthi, A. K., et al. 2022, *Solar Phys.*, 297(12), 153.
- Domingo, V., Fleck, B., & Poland, A. I. 1995, *Solar Phys.*, 162(1-2), 1.
- Fulara, A., Chandra, R., Chen, P. F., et al. 2019, *Solar Phys.*, 294(5), 56.
- Gopalswamy, N., Xie, H., Mäkelä, P., et al. 2013, *Adv. Space Res.*, 51(11), 1981.
- Guo, J. H., Ni, Y. W., Zhong, Z., et al. 2023, *ApJS*, 266(1), 3.
- Guo, Y., Erdélyi, R., Srivastava, A. K., et al. 2015, *ApJ*, 799(2), 151.
- Hamini, A., Auxepales, G., Birée, L., et al. 2021, *Journal of Space Weather and Space Climate*, 11, 57.
- Harvey, J. W., Bolding, J., Clark, R., et al. 2011, *AAS/Solar Physics Division Meeting*, 42, 17.45.
- Hou, Z., Tian, H., Wang, J.-S., et al. 2022, *ApJ*, 928(2), 98.
- Kaiser, M. L., Kucera, T. A., Davila, J. M., et al. 2008, *Space Sci. Revs*, 136(1-4), 5.
- Klein, K.-L., Musset, S., Vilmer, N., et al. 2022, *A&A*, 663, A173.
- Kouloumvakos, A., Papaioannou, A., Waterfall, C. O. G., et al. 2024, *A&A*, 682, A106.
- Kwon, R.-Y. & Vourlidas, A. 2017, *ApJ*, 836(2), 246.
- Kwon, R.-Y., Zhang, J., & Olmedo, O. 2014, *ApJ*, 794(2), 148.
- Lemen, J. R., Title, A. M., Akin, D. J., et al. 2012, *Solar Phys.*, 275(1-2), 17.
- Luna, M., Su, Y., Schmieder, B., et al. 2017, *ApJ*, 850(2), 143.
- Mavromichalaki, H., Paschalis, P., Gerontidou, M., et al. 2022, *Universe*, 8(7), 378.
- Mishev, A. L., Koldobskiy, S. A., Larsen, N., & Usoskin, I. G. 2024, *Solar Phys.*, 299(2), 24.
- Moreton, G. E. & Ramsey, H. E. 1960, *Pub. Astron. Soc. Pac.*, 72(428), 357.
- Muhr, N., Veronig, A. M., Kienreich, I. W., et al. 2014, *Solar Phys.*, 289(12), 4563.
- Nakariakov, V. M. & Ofman, L. 2001, *A&A*, 372, L53.
- Nitta, N. V., Liu, W., Gopalswamy, N., & Yashiro, S. 2014, *Solar Phys.*, 289(12), 4589.
- Papaioannou, A., Kouloumvakos, A., Mishev, A., et al. 2022, *A&A*, 660, L5.
- Pesnell, W. D., Thompson, B. J., & Chamberlin, P. C. 2012, *Solar Phys.*, 275(1-2), 3.
- Roberts, B., Edwin, P. M., & Benz, A. O. 1984, *ApJ*, 279, 857.
- Schmieder, B., Démoulin, P., & Aulanier, G. 2013, *Adv. Space Res.*, 51(11), 1967.
- Shen, Y., Chen, P. F., Liu, Y. D., et al. 2019, *ApJ*, 873(1), 22.
- Smerd, S. F., Sheridan, K. V., & Stewart, R. T. 1974 Newkirk, G. A., editor, *Coronal Disturbances*, 57, 389.
- Su, W., Guo, Y., Erdélyi, R., et al. 2018, *Sci. Rep.*, 8, 4471.
- Thompson, B. J., Gurman, J. B., Neupert, W. M., et al. 1999, *ApJL*, 517(2), L151.
- Thompson, B. J., Plunkett, S. P., Gurman, J. B., et al. 1998, *Geophys. Res. Lett.*, 25(14), 2465.
- Vasanth, V., Umapathy, S., Vršnak, B., et al. 2014, *Solar Phys.*, 289(1), 251.
- Vourlidas, A. & Ontiveros, V. 2009, Ao, X. & Burrows, G. Z. R., editors, *American Institute of Physics Conference Series*, 1183, 139.
- Warmuth, A. 2015, *Living Reviews in Solar Physics*, 12(1), 3.
- Warmuth, A. & Mann, G. 2005, *A&A*, 435(3), 1123.
- Zhang, Q. M., Chen, J. L., Li, S. T., et al. 2022, *Solar Phys.*, 297(2), 18.
- Zhukov, A. N. & Auchère, F. 2004, *A&A*, 427, 705.
- Zhukov, A. N., Rodriguez, L., & de Patoul, J. 2009, *Solar Phys.*, 259(1-2), 73.